Biol. Chem., Vol. 386, pp. 127–136, February 2005 • Copyright © by Walter de Gruyter • Berlin • New York. DOI 10.1515/BC.2005.016

# Pre-steady-state kinetic analysis of riboflavin synthase using a pentacyclic reaction intermediate as substrate

**Boris Illarionov[a], Ilka Haase, Markus Fischer, Adelbert Bacher and Nicholas Schramek***

Lehrstuhl für Organische Chemie und Biochemie, Technische Universität München, Lichtenbergstr. 4, D-85747 Garching, Germany

* Corresponding author
e-mail: nicholas.schramek@ch.tum.de

## Abstract

Riboflavin synthase catalyses a mechanistically complex dismutation affording riboflavin and 5-amino-6-ribitylamino-2,4(1*H*,3*H*)-pyrimidinedione from 6,7-dimethyl-8-ribityllumazine. A pentacyclic adduct (compound **2**) of two substrate molecules was used as substrate for pre-steady-state kinetic analysis. Whereas the wild-type enzyme catalyses the decomposition of compound **2** into a mixture of riboflavin and 5-amino-6-ribitylamino-2,4(1*H*,3*H*)-pyrimidinedione, as well as into two equivalents of 6,7-dimethyl-8-ribityllumazine, a H102Q mutant enzyme predominantly catalyses the former reaction. Stopped-flow experiments with this mutant enzyme failed to identify a reaction intermediate between compound **2** and riboflavin. However, the apparent rate constants for the formation of riboflavin as observed by stopped-flow and quenched-flow experiments were significantly different, thus suggesting that the reaction proceeds via a significantly populated intermediate, the absorbance of which is similar to that of compound **2**. An F2A mutant enzyme converts compound **2** predominantly into 6,7-dimethyl-8-ribityllumazine. Stopped-flow experiments using compound **2** as substrate indicated a slight and rapid initial increase in absorbance at 310 nm, followed by a slower decrease. This finding, in conjunction with different apparent rates for the formation of 6,7-dimethyl-8-ribityllumazine, suggests the involvement of a significantly populated intermediate in the transition between compound **2** and 6,7-dimethyl-8-ribityllumazine, the optical spectrum of which is similar to that of compound **1**.

**Keywords:** enzyme kinetics; flavines; pteridines; quenched flow; riboflavin biosynthesis; stopped-flow.

## Introduction

Riboflavin synthase catalyses a mechanistically complex dismutation affording riboflavin (**3**) and 5-amino-6-ribitylamino-2,4(1*H*,3*H*)-pyrimidinedione (**4**) from 6,7-dimethyl-8-ribityllumazine (**1**), (Figure 1; Plaut, 1963; Harvey and Plaut, 1966); for reviews see also Plaut and Beach (1967), Plaut et al. (1974), Bacher and Mailänder (1976), Bacher (1991) and Bacher et al. (1996, 2000). The reaction involves the exchange of a four-carbon unit between one substrate molecule acting as donor and a second substrate molecule acting as acceptor (Plaut, 1963; Harvey and Plaut, 1966). Recent studies showed that the enzyme initially produces a pentacyclic adduct (compound **2**) from two molecules of 6,7-dimethyl-8-ribityllumazine (Illarionov et al., 2001a). Compound **2** can be fragmented by riboflavin synthase in two different ways, affording either two molecules of 6,7-dimethyl-8-ribityllumazine (reverse reaction) or one molecule each of riboflavin and 5-amino-6-ribitylamino-2,4(1*H*,3*H*)-pyrimidinedione (forward reaction). Moreover, the pentacyclic intermediate was found to fulfil the criteria for a kinetically competent reaction intermediate (Illarionov et al., 2001a). Pre-steady-state kinetic experiments were well in line with the formation of the pentacyclic adduct as a reaction intermediate (Illarionov et al., 2003).

Riboflavin synthases of eubacteria, plants and fungi are homotrimers of subunits with a mass of approximately 25 kDa. The N- and C-terminal portions of the subunit show marked sequence similarity (Schott et al., 1990). In line with that finding, X-ray structure analysis has shown that each subunit folds into two domains with closely similar folding topology (Eberhardt et al., 2001; Liao et al., 2001; Truffault et al., 2001; Meining et al., 2003). Each domain forms a shallow surface cavity, which can accept one molecule of 6,7-dimethyl-8-ribityllumazine. The enzyme-catalysed reaction is believed to occur at the interface of the N-terminal domain of one subunit and the C-terminal domain of an adjacent subunit of the homotrimeric enzyme (Gerhardt et al., 2002). The two cooperating subunits form a pseudo-$c_2$-symmetric ensemble, the topological features of which are in line with earlier studies on the regiochemistry of the enzyme-catalysed reaction (Beach and Plaut, 1970; Sedlmaier et al., 1987; Römisch et al., 2002) which had already suggested a $c_2$-symmetrical arrangement for the substrate molecules at the active site (Schott et al., 1990). The C-terminal domain is believed to accommodate the substrate molecule serving as donor and the N-terminal domain is believed to accommodate the substrate molecule serving as acceptor (Gerhardt et al., 2002).

Surprisingly, the homotrimeric riboflavin synthase of *Escherichia coli* does not obey trigonal symmetry (Liao et al., 2001), and it appears that only one C-terminal domain and one N-terminal domain contact each other in a topologically appropriate way for the dismutation to occur (Liao et al., 2001). However, it has been suggested that structural fluctuations of the protein could enable all six domains of the homotrimer to become sequentially

[a] On leave of absence from the Institute for Biophysics, 660036 Krasnoyarsk, Russia.

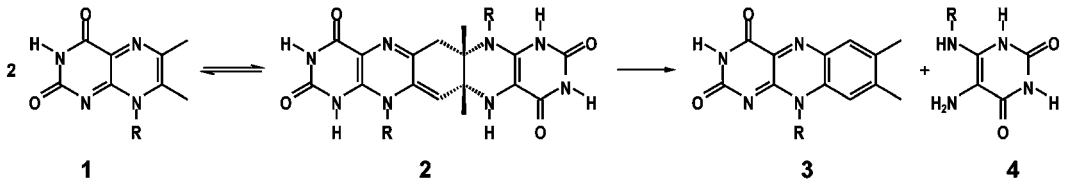

**Figure 1** Reaction catalysed by riboflavin synthase. R, ribityl.

involved in catalysis (Gerhardt et al., 2002; Illarionov et al., 2003).

Surprisingly, most mutations of amino acid residues in the first shell of the active site had relatively little impact on enzyme catalysis (Illarionov et al., 2001b). On the other hand, certain mutations of N-terminal amino acids located in the second shell with respect to the substrate binding site of the N-terminal domains have a major impact on the catalytic activity of the enzyme.

We have used the pentacyclic reaction intermediate, compound **2**, as the substrate for pre-steady-state experiments using wild-type and mutant riboflavin synthases in order to study the complex reaction trajectory in closer detail.

## Results

The riboflavin synthase mutant H102Q converts 6,7-dimethyl-8-ribityllumazine into riboflavin with very low catalytic activity (<0.4% compared to the wild-type enzyme) (Illarionov et al., 2001b). On the other hand, steady-state experiments showed that the reaction intermediate, compound **2,** is used more efficiently as substrate (Table 1), and the formation of **2** from **1** is clearly the rate-limiting step of the overall reaction. Therefore, the mutant appeared appropriate for pre-steady-state kinetic analysis of the second part of the riboflavin synthase trajectory, i.e., the conversion of compound **2** into a mixture of riboflavin and 5-amino-6-ribitylamino-2,4(1*H*,3*H*)-pyrimidinedione without concomitant formation of **1** in significant amounts (Figure 1).

Quenched-flow experiments were carried out with reaction mixtures containing the H102Q mutant enzyme and compound **2** at a molar ratio of 0.95:1 (substrate per protein subunit). The reaction mixtures were incubated at 25°C and were quenched by the rapid addition of 0.3 M hydrochloric acid. Riboflavin, compound **2** and 6,7-dimethyl-8-ribityllumazine were determined by HPLC [since 5-amino-6-ribitylamino-2,4(1*H*,3*H*)-pyrimidinedione and riboflavin are formed at a molar ratio of 1:1, the determination of riboflavin was sufficient]. During a period of 50 s, 50% of the proffered compound **2** was consumed (Figure 2A). Concomitantly, riboflavin was formed in nearly stoichiometric amounts. The amount of 6,7-dimethyl-8-ribityllumazine formed was very low (<4% compared to riboflavin). A control experiment (data not shown) confirmed that 6,7-dimethyl-8-ribityllumazine (**1**) is consumed by the mutant enzyme at a much slower rate (approximately 12 min for 50% depletion), in line with our earlier finding that compound **2** is a kinetically competent reaction intermediate.

**Table 1** Riboflavin formation under steady-state conditions.

| Protein | Turnover number ($min^{-1}$)[a] | |
|---|---|---|
| | From **1** | From **2** |
| Wild type | 16±2.6 | 44±8 |
| F2A | <0.001 | 0.013±0.005 |
| H102Q | 0.061±0.02 | 1.2±0.3 |

[a] Per enzyme trimer.

In an earlier study, we found the following reaction scheme to be appropriate for the evaluation of stopped-flow data using 6,7-dimethyl-8-ribityllumazine as substrate (Illarionov et al., 2003):

$$2\ \text{Compound}\ \mathbf{1} \underset{k_2}{\overset{k_1}{\rightleftharpoons}} \text{Compound}\ \mathbf{2} \xrightarrow{k_3} \text{Compound}\ \mathbf{3} + \text{Compound}\ \mathbf{4} \quad (1)$$

Since, in the present experiments with the mutant, the amount of **1** was quite low at all times and, moreover, the conversion of **1** into **2** is a very slow reaction, it appears justified to simplify reaction scheme (1) as follows:

$$2\ \text{Compound}\ \mathbf{1} \xleftarrow{k_2} \text{Compound}\ \mathbf{2} \xrightarrow{k_3} \text{Compound}\ \mathbf{3} + \text{Compound}\ \mathbf{4} \quad (2)$$

Using reaction scheme (2), numerical simulation of the data shown in the Figure 2A afforded apparent first-order rate constants of 0.00027 $s^{-1}$ ($k_2$) and 0.013 $s^{-1}$ ($k_3$) (Table 2). The deviation between the fit and the experimental data (Figure 2A) is analysed in closer detail in the Discussion section in connection with the stopped-flow experiments described below.

The optical spectra of the known reactants in the riboflavin synthase trajectory extend over a wide wavelength range (up to approx. 530 nm) (Figure 3). Notably, the spectrum of riboflavin extends further into the long-wavelength range than any of the other known participants in the reaction; hence, its formation can be diagnosed in the long-wavelength range without substantial contributions from earlier reaction components.

Under the conditions of stopped-flow experiments, which require a relatively high concentration of enzyme and substrate, the reactants are predominantly present in protein-bound form, and therefore their absorbance bands are shifted by the protein environment. Specifically, the lowest energy $\pi\pi^*$ transition of riboflavin is shifted from 445 to 453 nm, and the lowest energy $n\pi^*$ transition is shifted from 370 to 385 nm, as shown by analysis of a stoichiometric mixture of riboflavin synthase

with riboflavin and **4** (Figure 3, Table 3). The spectra of protein-bound 6,7-dimethyl-8-ribityllumazine and compound **2** cannot be obtained from steady-state measurements because they are catalytically converted by the enzyme; however, they can be obtained from the stopped-flow experiments described below.

A series of optical spectra from a typical stopped-flow experiment using H102Q mutant protein and compound **2** as substrate is shown in Figure 4A. The substrate was proffered at a molar ratio of 0.9:1 (substrate per protein subunit). Selected spectra from that series are also shown superimposed in Figure 5A. Concomitantly with the monotonic decrease in the characteristic maximum of compound **2** at 310 nm, the characteristic absorbance bands of enzyme-bound riboflavin at 453, 385 and 272 nm appear. The intersections between the spectra in Figure 5A are reminiscent of isobestic points; upon closer examination, however, that view is not confirmed.

For a more detailed analysis, the data set in Figure 4A was subjected to single value decomposition using the program SPECFIT/32 3.0.34. Since the formation of 6,7-dimethyl-8-ribityllumazine by the mutant protein was shown to be minimal in the previous quenched-flow experiments (Table 2), reaction scheme (2) can be simplified further as follows:

$$\text{Compound } \mathbf{2} \xrightarrow{k_3} \text{Compound } \mathbf{3} + \text{Compound } \mathbf{4} \qquad (3)$$

The reconstructed absorbance spectra are shown in Figure 6A. The dotted line resembles the spectrum of a stoichiometric mixture of riboflavin and 5-amino-6-ribitylamino-2,4(1*H*,3*H*)-pyrimidinedione complexed with the protein (cf. Figure 3). The solid line in Figure 6A resembles the spectrum of compound **2** in solution (cf. Figure 3) and is believed to represent this compound complexed with the protein. The reaction progress as shown in Fig 6B indicates a monotonous decrease in the substrate-type spectrum and a monotonous increase in the spectrum attributed to a protein-bound mixture of the two products, i.e., riboflavin (**3**) and 5-amino-6-ribitylamino-2,4(1*H*,3*H*)-pyrimidinedione (**4**). Notably, the sum of the concentrations of compound **2** and riboflavin is constant throughout the experiments within the limits of experimental accuracy.

Linear deconvolution failed to uncover absorbance contributions from any hitherto unknown intermediate. This agrees with the result of the quenched-flow experiments, in which HPLC analysis of the quenched reaction mixtures also failed to detect any species beside those mentioned above. Surprisingly, however, the time required for 50% consumption of compound **2** was approximately 100 s in stopped-flow experiments, whereas quenched-flow experiments under the same experimental conditions took approximately 50 s (Figure 6C).

The long-wavelength absorbance of riboflavin is highly characteristic, and interpretation of the stopped-flow experiments with regard to the time course of riboflavin formation therefore appears uncontroversial. In the quenched-flow experiment, on the other hand, the composition of the mixtures used for HPLC analysis could have been modified by acid quenching. More specifically,

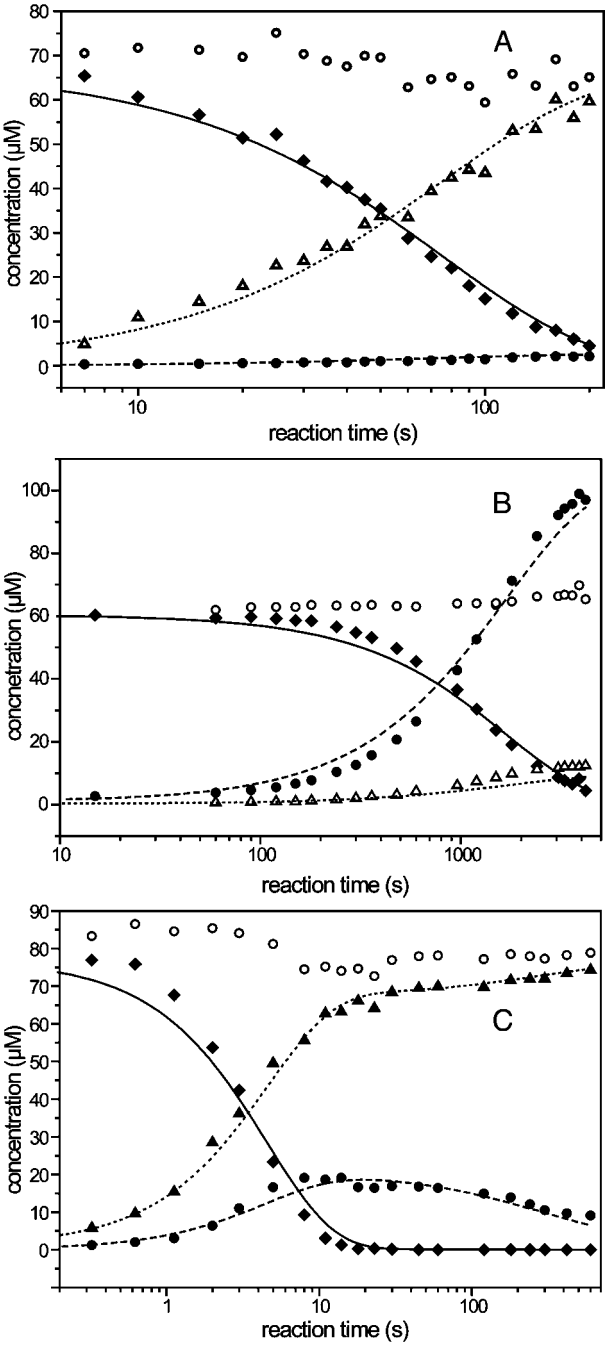


**Figure 2** Quenched-flow kinetics of riboflavin synthase using compound **2** as substrate.
Reaction mixtures containing 150 mM potassium phosphate, pH 6.9, 2 mM dithiothreitol (DTT), 60–80 μM compound **2**, and riboflavin synthase in a molar ration of 0.95:1 (substrate per protein subunit) were incubated at 25°C. Experimental values for concentrations are indicated as follows: ●, 6,7-dimethyl-8-ribityllumazine; ♦, compound **2**; △, riboflavin. Numerical simulations of experimental data were carried out using reaction scheme (2). Results are summarised in Table 2. The optimised concentration profiles are represented as lines. (A) Reaction of H102Q mutant. (B) Reaction of F2A mutant. (C) Reaction of wild-type riboflavin synthase.

the acid treatment could have converted a hitherto unknown intermediate into riboflavin. These aspects are considered in more detail in the discussion section.

Earlier steady-state kinetic experiments had shown that the replacement of Phe-2 has a strong impact on

the catalytic rate of riboflavin synthase, although the amino acid residue is not in direct contact with the ligand (it is in fact located in the second shell with respect to the active site) (Illarionov et al., 2001b; Gerhardt et al., 2002). Specifically, even a minor substitution, such as tyrosine for phenylalanine at position 2, has been shown to lead to the formation of riboflavin at a substantially lower rate compared to the wild type. The F2A mutant did not form detectable amounts of riboflavin during incubation with compound **1** for 90 min. However, the F2A mutant can convert compound **2** into 6,7-dimethyl-8-ribityllumazine at a low, but detectable rate (Table 2).

N-Terminal Edman degradation of various riboflavin synthase mutant proteins indicated that the replacement of Phe-2 by alanine is conducive to proteolytic removal of the start methionine in the recombinant *E. coli* host, whereas other protein variants retain the N-terminal methionine (for a review of this phenomenon, see Giglione et al., 2004).

Optical spectra from typical stopped-flow experiments with the F2A mutant and compound **2** as substrate are shown in Figure 4B, for which compound **2** and enzyme were mixed at a ratio of 0.9 mol substrate per mol of protein subunit. For closer inspection, selected absorbance traces are shown in Figure 7A, and absorbance values at selected wavelengths versus time are shown in Figure 7B.

At 310 nm, compound **2** has a strong absorbance maximum, whereas 6,7-dimethyl-8-ribityllumazine, riboflavin and the pyrimidine **4** have much lower absorbance coefficients. Hence, we would expect the absorbance at that wavelength to decrease monotonously if no other species with high absorbance at 310 nm were involved in the trajectory. In contrast to the expected monotonous decrease, Figure 7B shows a slight initial increase in absorbance at 310 nm, extending over a period of approximately 100 s (cf. insets in Figure 7A,B). This implies that an unknown molecular species (different from compounds **1**, **2** and **3**) contributes to the absorbance at 310 nm.

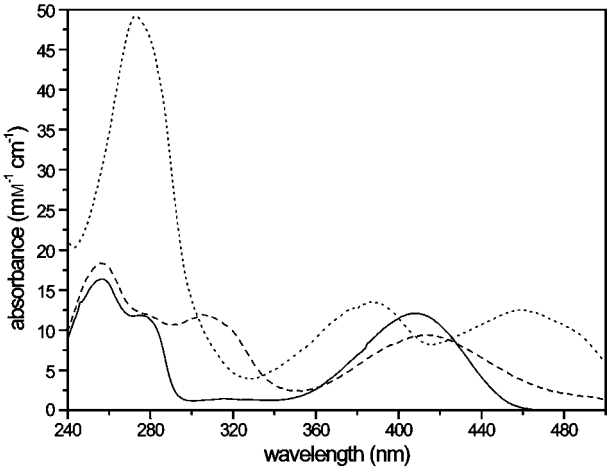


**Figure 3** Optical spectra of compounds supposed to occur in the reaction trajectory of riboflavin synthase.
6,7-Dimethyl-8-ribityllumazine, solid line; compound **2**, dashed line; enzyme-bound mixture of riboflavin and 5-amino-6-ribitylamino-2,4(1*H*,3*H*)-pyrimidinedione, dotted line. All spectra were recorded in 150 mM potassium phosphate, pH 6.9, containing 2 mM DTT.

**Table 2** Kinetic constants obtained from single turnover quenched-flow experiments using reaction scheme (1) or (2), respectively, for numerical simulation of experimental data.

| Protein | Substrate | $k_1$ ($s^{-1}$ $\mu M^{-1}$) | $k_2$ ($s^{-1}$) | $k_3$ ($s^{-1}$) |
|---|---|---|---|---|
| Wild type | **1**[a] | 0.0048±0.0008 | 0.06±0.007 | 0.29±0.03 |
| | **2** | 0.002±0.0004 | 0.03±0.0016 | 0.35±0.01 |
| F2A | **1** | <0.000001 | ND[b] | ND[b] |
| | **2** | <0.000001 | 0.0005±0.00002 | 0.00007±0.00001 |
| H102Q | **1** | 0.000003±0.000001 | ND[c] | ND[c] |
| | **2** | <0.00001 | 0.00027±0.0001 | 0.013±0.0002 |

[a]Taken from Illarionov et al. (2003).
[b]The respective values could not be determined because practically no compound **2** was formed from **1** by the F2A under the experimental conditions used in this study.
[c]The concentration of **2** was extremely low in the course of this experiment. Hence, $k_2$ and $k_3$ values could not be determined by regression analysis with reasonable precision.

**Table 3** Absorption maxima for compounds and optical transients occurring in the reaction trajectory of riboflavin synthase (150 mM potassium phosphate, pH 6.9, and 2 mM DTT).

| | $\lambda_1$ (nm) | $\lambda_2$ (nm) | $\lambda_3$ (nm) | $\lambda_4$ (nm) |
|---|---|---|---|---|
| Compound **1** | 256 | 276 | – | 408 |
| Transient A | 257 | 279 | 318 | 409 |
| Compound **2** | 256 | 279 | 306 | 415 |
| Transient B | 254 | 280 | 308 | 415 |
| Compound **3** | 266 | 370 | 445 | |
| Compound **3**, enzyme-bound | 272 | 385 | 453 | |
| Compound **4** | 284 | | | |
| Compound **4**, enzyme-bound | 278 | | | |
| Transient C | 272 | 385 | 454 | |

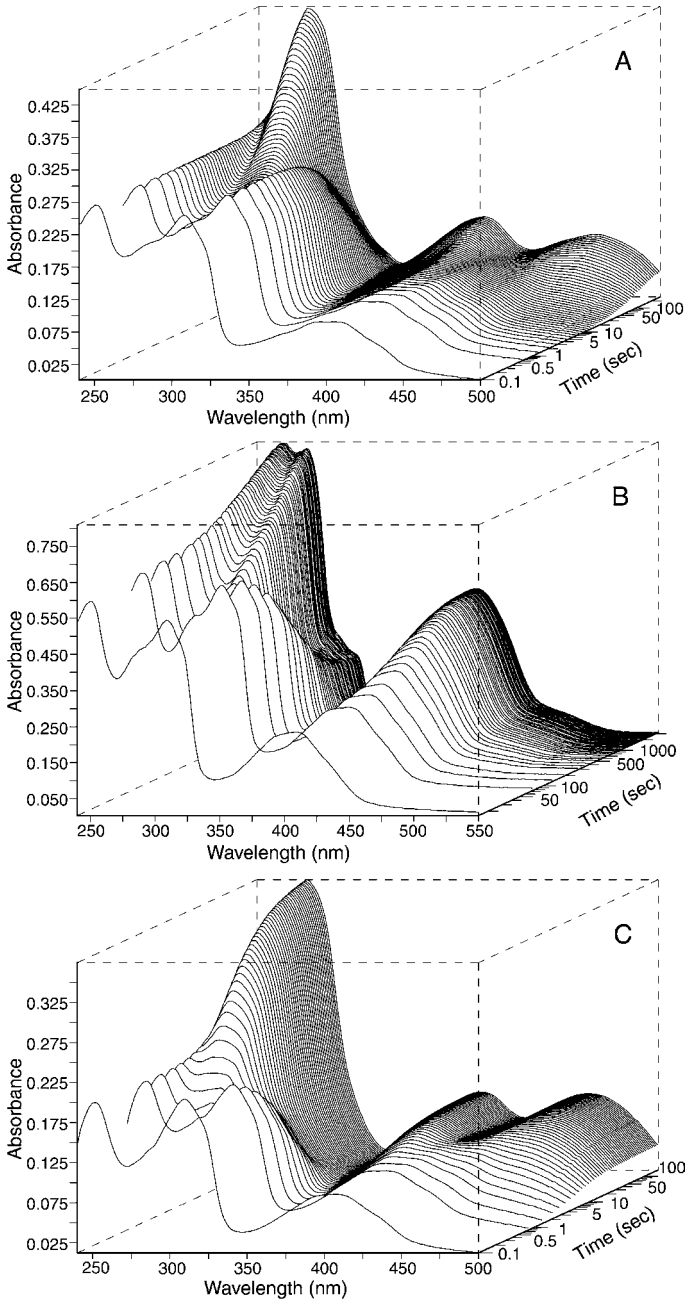


**Figure 4** Optical spectra from single turnover stopped-flow experiments with riboflavin synthase using compound **2** as substrate. Experiments were carried out at 25°C in 150 mM potassium phosphate, pH 6.9, containing 2 mM DTT (reaction buffer). Absorption spectra were recorded at intervals of 100 ms (wild-type enzyme and H102Q mutant) and 15 s (F2A mutant). (A) H102Q mutant of riboflavin synthase. The concentrations were 72 μM enzyme subunits and 65 μM compound **2** in reaction buffer. (B) F2A mutant of riboflavin synthase. The concentrations were 180 μM enzyme subunits and 166 μM compound **2** in reaction buffer. (C) Wild-type riboflavin synthase using compound **2** as substrate. The concentrations were 62 μM enzyme subunits and 57 μM compound **2** in reaction buffer.

For a more detailed analysis, the data set in Figure 4B was subjected to singular value decomposition. Since the F2A mutant did not convert compound **1** to riboflavin or compound **2**, and the formation of riboflavin from compound **2** is very slow, the simplification of reaction scheme (1) was justified, as follows:

$$2\ \text{Compound}\ \mathbf{1} \xleftarrow{k_2} \text{Compound}\ \mathbf{2} \qquad (4)$$

The reconstructed absorbance spectra are shown in Figure 8A. The concentration curves for these molecular species are shown in Figure 8B. However, it was not possible to resolve the spectrum of the unknown molecular species by linear deconvolution, probably because its absorption spectrum is not sufficiently different from that of compound **2**.

A quenched-flow experiment with the F2A mutant and compound **2** as substrate is shown in Figure 2B. HPLC

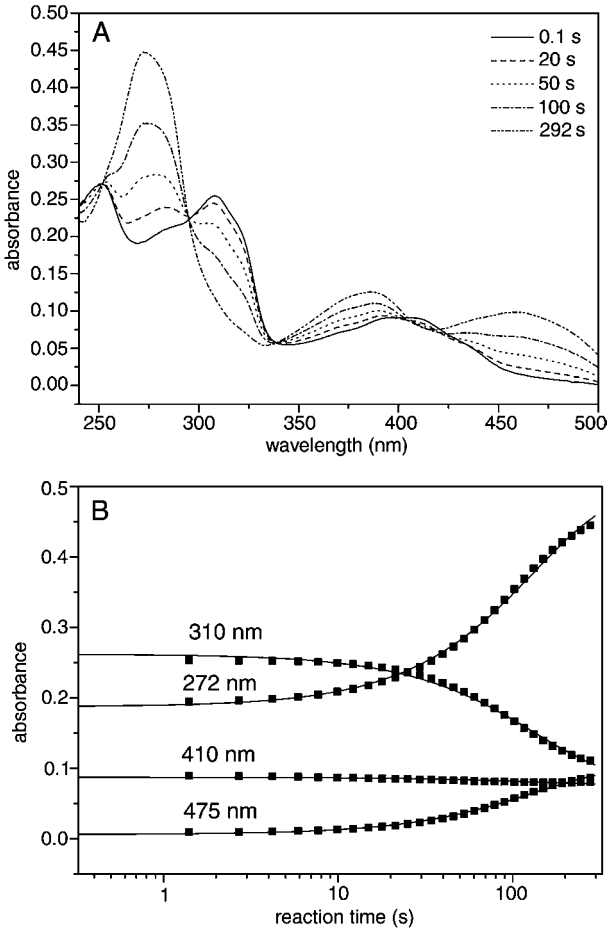


**Figure 5** Single turnover stopped-flow experiment of H102Q mutant of riboflavin synthase.
(A) Selected spectra from the single turnover experiment shown in Figure 4A. (B) Absorbance changes observed during the single turnover stopped-flow experiment shown in Figure 4A. Symbols represent experimental data. Solid lines represent numerical simulation using the kinetic constant given in Table 4.

analysis of the quenched samples detected compound **2**, riboflavin and 6,7-dimethyl-8-ribityllumazine, but no other component with significant absorbance above 320 nm. Moreover, the stoichiometry of the components appeared balanced throughout the reaction interval. On the other hand, an attempt to fit the data to reaction scheme (1) reveals appreciable deviations between the experimental data and the expected concentrations of **1**, **2,** and **3** if it is assumed that conversion of **2** to **1** is controlled by a single exponential process. Moreover, it should be noted that the apparent rate constants for product formation are significantly different in the stopped-flow and quenched-flow experiments (cf. Figure 8C). As discussed in more detail below, this is best explained by assuming an intermediate between compounds **2** and **1**, the spectrum of which resembles that of compound **1** and which is converted into compound **2** by acid treatment.

For the sake of completeness, we also carried out both stopped-flow and quenched-flow experiments using wild-type riboflavin synthase and compound **2** as substrate (Figures 2C and 4C; Table 2). The landscape of the optical spectra shown in Figure 4C is qualitatively similar to the data obtained with the H102Q mutant (Figure 4A). It is not surprising in light of the difficulties reported with the mutants, which have simpler reaction trajectories, that these data could not be satisfactorily resolved by numerical deconvolution. Thus, these data are only presented to show the relationship between the overall reaction rates of the proteins. With respect to the quenched-flow experiment, the regression analysis revealed significant deviations of the experimental data from those expected during the first 2 s of the experiment (Figure 2C). This suggests that in the early phase of the experiment, compound **2** may undergo rapid transformations that are not considered in reaction scheme (1).

## Discussion

The formation of riboflavin and 5-amino-6-ribitylamino-2,4(1*H*,3*H*)-pyrimidinedione from 6,7-dimethyl-8-ribityllumazine involves the transfer of a four-carbon moiety between two identical, heterocyclic substrate molecules that can be formally described as a dismutation. However, the reaction is obviously different from typical dismutation reactions in view of the much higher mechanistic complexity.

Surprisingly, this unusual reaction can proceed in the absence of catalysts by boiling anaerobic aqueous solutions under neutral or acidic conditions (Rowan and Wood, 1963; Paterson and Wood, 1972). It was also shown that the enzyme-catalysed and uncatalysed reactions proceed with the same regiospecificity. On the other hand, the reaction rates of riboflavin synthase are rather modest. Riboflavin synthases typically catalyse approximately less than 10 turnovers per minute and per subunit.

More than three decades ago, several mechanistic alternatives were proposed for this reaction sequence by Wood, Plaut and their co-workers (Rowan and Wood, 1963, 1968; Beach and Plaut, 1969). An initial hypothesis suggesting the parallel arrangement of two lumazine substrates in the activated complex was later modified in favour of an anti-parallel arrangement on the basis of regiochemical data (Paterson and Wood, 1969). Later, Beach and Plaut suggested intermediates of the form of tricyclic molecules generated by the covalent addition of side-chain hydroxyl groups to the position-7 carbon of 6,7-dimethyl-8-ribityllumazine (Plaut and Beach, 1967; Beach and Plaut, 1970).

**Table 4** Kinetic constants obtained from single turnover stopped-flow experiments using reaction schemes (3) and (4) for numerical simulation.

| Protein | Substrate | $k_1$ ($s^{-1}$) | $k_2$ ($s^{-1}$) | $k_3$ ($s^{-1}$) |
|---|---|---|---|---|
| H102Q | **2** | – | – | 0.00743±0.00007 |
| F2A | **2** | – | 0.00132±0.00003 | – |

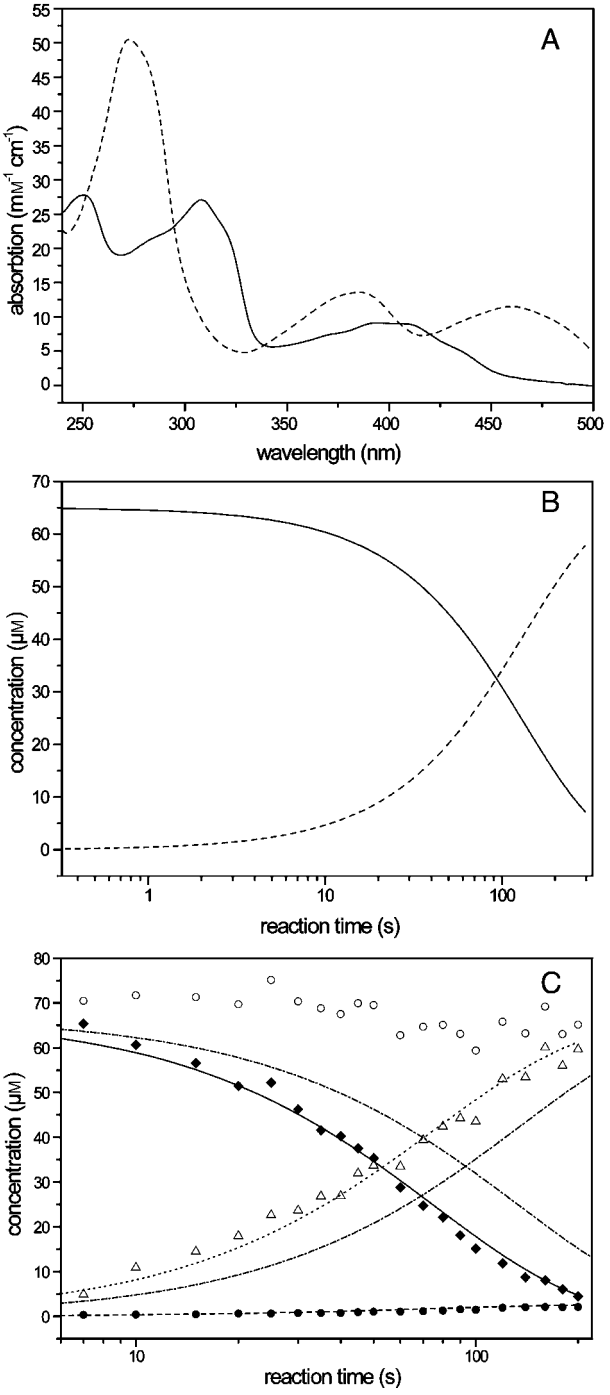


**Figure 6** Numerical simulation of stopped-flow data shown in Figure 4A.
Numerical simulation was carried out using reaction scheme (3). Solid lines, compound **2**; dashed lines, mixture of compounds **3** and **4**. (A) Reconstructed absorbance of transient chromophores. (B) Concentration of transient species afforded by numerical analysis. (C) Superimposition of Figures 2A and 6B.

Figure 9 shows a hypothetical reaction sequence that combines the essential aspects of the mechanisms originally suggested by Plaut, Wood and their co-workers with the new findings on the pentacyclic reaction intermediate, compound **2** (Illarionov et al., 2001a). This hypothetical mechanism, which has been discussed in some detail earlier, implicates several hypothetical intermediates prior to, as well as posterior to, compound **2**. The present study was initiated as an attempt to document any of these hypothetical structures. Since the kinetic analysis is complicated by the bidirectional nature of the reaction, i.e., the simultaneous formation of riboflavin, 5-amino-6-ribitylamino-2,4(1*H*,3*H*)-pyrimidinedione and 6,7-dimethyl-8-ribityllumazine from compound **2**, most of the work was carried out with mutant enzymes, which preferentially catalyse the conversion of compound **2** into 6,7-dimethyl-8-ribityllumazine or, alternatively, into a mixture of riboflavin and 5-amino-6-ribitylamino-2,4(1*H*,3*H*)-pyrimidinedione, albeit at lower rates compared to the wild-type enzyme.

Although numerical deconvolution of the stopped-flow experiments, as well as the HPLC analysis of acid-quenched reaction mixtures, failed to directly demonstrate the formation of any hitherto unknown intermediates, there is significant circumstantial evidence that supports the involvement of intermediates in both the upstream and downstream parts of the reaction trajectory. (i) The stopped-flow and quenched-flow experiments afford different apparent rate constants for the formation of riboflavin from compound **2** by the H102Q mutant protein. (ii) Similarly, the stopped-flow and quenched-flow experiments afford different apparent rate constants for the

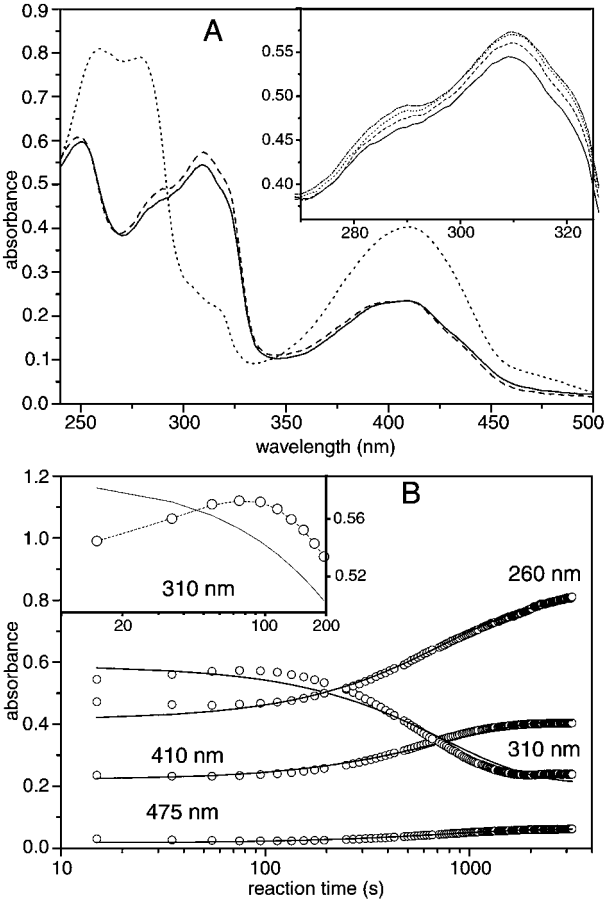


**Figure 7** Single turnover stopped-flow experiment of the F2A mutant of riboflavin synthase.
(A) Selected spectra from the single turnover experiment shown in Figure 4B. (B) Absorbance changes observed during the single turnover stopped-flow experiment shown in Figure 4B. Symbols represent experimental data. Solid lines represent numerical simulation using the kinetic constant values shown in Table 4.

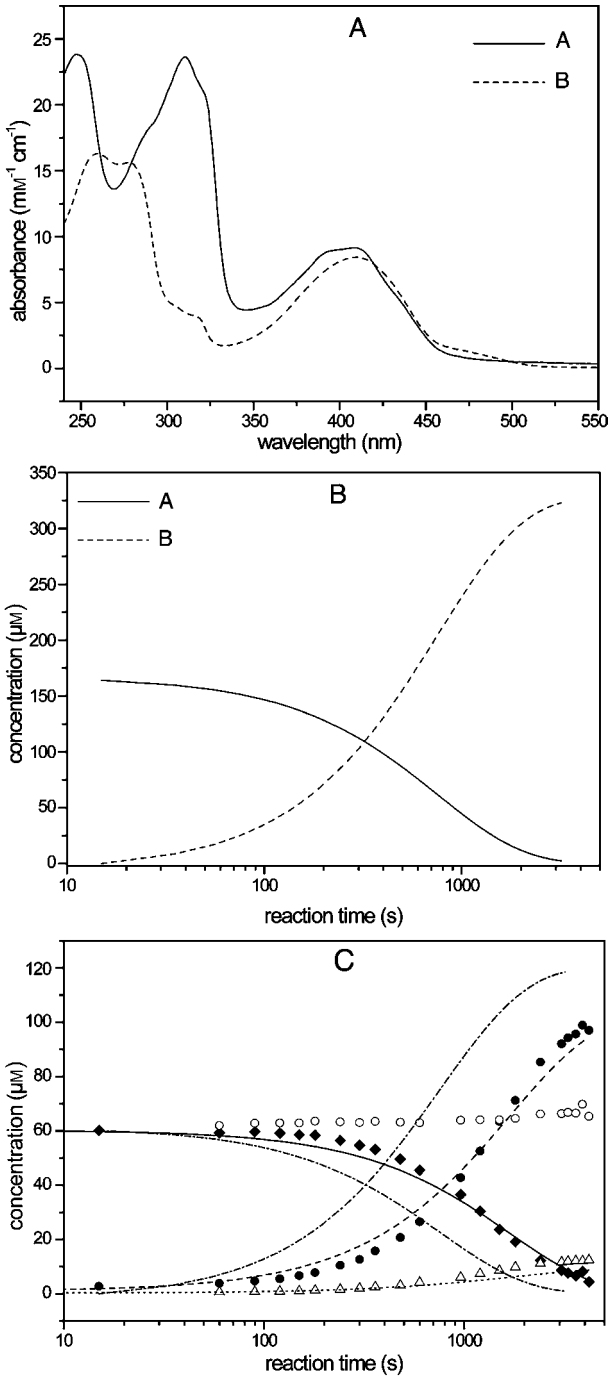


**Figure 8** Numerical simulation of stopped-flow data shown in Figure 4B.
Numerical simulation was carried out using reaction scheme (4). Solid lines, compound **2**; dashed lines, compound **1**. (A) Reconstructed absorbance of transient chromophores. (B) Concentration of transient species afforded by numerical analysis. (C) Superimposition of Figures 2B and 8B.

conversion of compound **2** into 6,7-dimethyl-8-ribityllumazine by the F2A mutant protein. (iii) A monotonous decrease in absorbance at 310 nm would have been expected for the experiment with the F2A mutant if only **1**, **3,** and **4** (which have lower absorbance values at that wavelength compared to compound **2**) were involved; contrary to that hypothesis, we observe a shallow maximum absorbance at 310 nm after approximately 100 s. (iv) Simulation of the quenched-flow experiments using single-exponential rate constants shows significant deviations for the experimental data, which indicates that more complex algorithms via additional intermediates may be required.

Several possible candidates for the intermediates that may have gone undetected in the optical experiments can be derived from inspection of the hypothetical reaction mechanism shown in Figure 9. For example, the $\pi$ electron system of adduct **6** resembles that of 6,7-dimethyl-8-ribityllumazine in the neutral form, and the spectrum of the two compounds in the long-wavelength range are likely to be quite similar. Under this assumption, if **6** were significantly populated at any time in the reaction trajectory, it would hardly be detected by single value decomposition. Moreover, if acid treatment of **6** were conducive to the regeneration of compound **2** rather than to the formation of 6,7-dimethyl-8-ribityllumazine, only the quenched-flow experiments would realistically describe the formation of 6,7-dimethyl-8-ribityllumazine, whereas optical detection would misinterpret the formation of intermediate **6** as the formation of 6,7-dimethyl-8-ribityllumazine. Similarly, compound **9** could be a significantly populated intermediate in the late part of the reaction trajectory that is converted to **3** and **4** by acid quenching.

## Materials and methods

### Materials

6,7-Dimethyl-8-ribityllumazine was synthesised by published procedures (Bacher et al., 1997). Compound **2** was prepared as previously described (Illarionov et al., 2001a).

### Bacterial strains

Recombinant *E. coli* BL21(DE3) strains expressing the *E. coli* wild-type riboflavin synthase or its mutant variants have been previously described (Illarionov et al., 2001b).

### Protein purification

Recombinant wild-type and mutant riboflavin synthase were purified using published procedures (Illarionov et al., 2003).

### Stopped-flow kinetic experiments

Experiments were carried out using an SFM4/QS apparatus from Bio-Logic (Claix, France) equipped with a linear array of three mixers and four independent syringes. The contents of a 1.5-mm-light-path quartz cuvette behind the last mixer were monitored using a Tidas diode array spectrophotometer (200–610 nm) equipped with a 15-W deuterium lamp as light source (J&M Analytische Meß- und Regeltechnik, Aalen, Germany). The reaction buffer contained 150 mM potassium phosphate, pH 6.9, and 2 mM dithiothreitol (DTT). The enzyme solution was mixed with substrate solution at a ratio of 1:1 at a temperature of 25°C and a total flow rate of 4 ml $s^{-1}$. The calculated dead time was 7.6 ms. Spectra integrated over 96 ms were recorded at intervals of 100 ms.

### Quenched-flow kinetics

The mixing apparatus described above was equipped with a computer-controlled valve instead of an optical cuvette. A delay loop with a nominal volume of 230 μl was filled with reactants at a temperature of 25°C and a total flow rate of 4 ml $s^{-1}$. At the

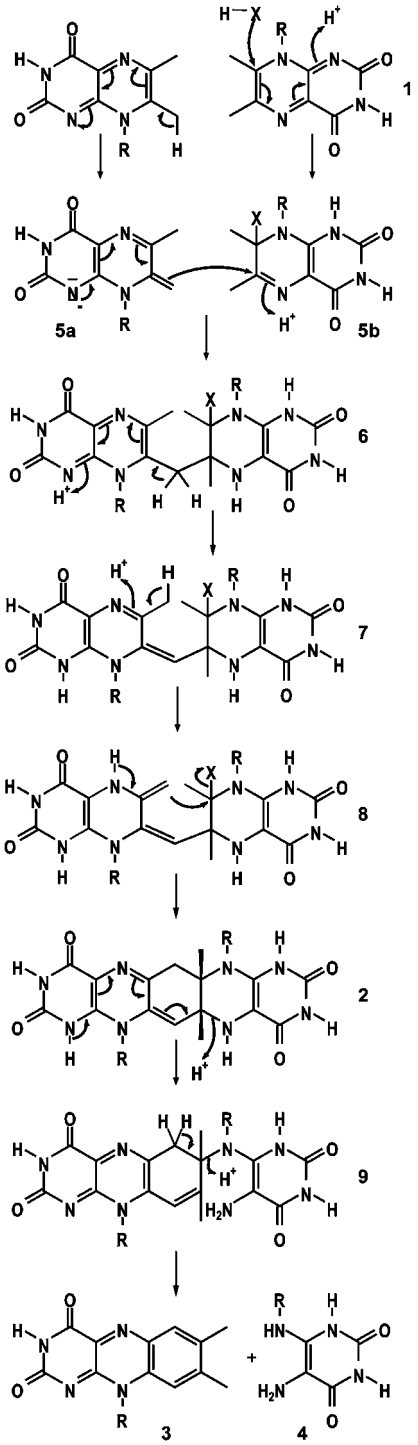

**Figure 9** Hypothetical reaction mechanism for riboflavin synthase (Paterson and Wood, 1972; Plaut et al., 1974; Bacher, 1991; Illarionov et al., 2001a).
R, ribityl; X, unknown nucleophile.

times indicated, the reaction mixtures in the delay loop were mixed at a 1:1 ratio with 0.3 M hydrochloric acid at a flow rate of 4 ml $s^{-1}$. Trichloroacetic acid was added to a final concentration of 50 mM and the samples were centrifuged (15 000 *g* for 10 min). The supernatant was stored at -80°C until further analysis.

### High-performance liquid chromatography

Experiments were carried out on a column of Hypersil RP 18 (4×250 mm; Schambeck, Bad Honnef, Germany) at a flow rate of 1.5 ml $min^{-1}$. An eluent containing methanol/formic acid/water (25:1:288, by volume) was used for determination of 6,7-dimethyl-8-ribityllumazine (retention volume, 6.5 ml) and compound **2** (retention volume, 7.4 ml). An eluent containing 0.1 M ammonium formate and 40% methanol (v/v) was used for determination of riboflavin (retention volume, 2.2 ml). The effluent was monitored using a diode array photometer.

### Global analysis of data from stopped-flow experiments

Prior to data analysis, the absorbance background caused by the enzyme was removed by subtraction of a blank data set obtained without the addition of substrate. Data reduction and stronger weighting of early spectra were achieved by extracting 300 spectra on a pseudo-logarithmic time base from the difference data sets. These data sets were then analysed using the program SPECFIT/32 3.0.30 (Spectrum Software Associates, Marlborough, USA).

### Analysis of data from quenched-flow experiments

Data sets were analysed using the DynaFit program (Kuzmic, 1996).

## Acknowledgments

This work was supported by grants from the Deutsche Forschungsgemeinschaft, the Fonds der Chemischen Industrie and the Hans-Fischer-Gesellschaft. We thank Dr. Peter Köhler for amino acid sequencing.

## References

Bacher, A. (1991). Biosynthesis of flavins. In: Chemistry and Biochemistry of Flavoenzymes, Vol. 1, F. Müller, ed. (Boca Raton, USA: CRC Press), pp. 215–259.

Bacher, A., and Mailänder, B. (1976). Biosynthesis of riboflavin. Structure of the purine precursor and origin of the ribityl side chain. In: Flavins and Flavoproteins, T.P. Singer, ed. (Amsterdam, The Netherlands: Elsevier), pp. 733–736.

Bacher, A., Eberhardt, S., and Richter, G. (1996). Biosynthesis of riboflavin. In: *Escherichia coli* and *Salmonella typhimurium*, Vol. 1, F.C. Neidhardt, J.L. Ingraham, K.B. Low, B. Magasanik, M. Schaechter, and H.E. Umbarger, eds. (Washington, DC, USA: American Society for Microbiology), pp. 657–664.

Bacher, A., Eberhardt, S., Fischer, M., Mörtl, S., Kis, K., Kugelbrey, K., Scheuring, J., and Schott, K. (1997). Biosynthesis of riboflavin: lumazine synthase and riboflavin synthase. Methods Enzymol. *280*, 389–399.

Bacher, A., Eberhardt, S., Fischer, M., Kis, K., and Richter, G. (2000). Biosynthesis of vitamin B2 (riboflavin). Annu. Rev. Nutr. *20*, 153–167.

Beach, R., and Plaut, G.W. (1969). The formation of riboflavin from 6,7-dimethyl-8-ribityllumazine in acid media. Tetrahedron Lett. *40*, 3489–3492.

Beach, R.L., and Plaut, G.W. (1970). Stereospecificity of the enzymatic synthesis of the o-xylene ring of riboflavin. J. Am. Chem. Soc. *92*, 2913–2916.

Eberhardt, S., Zingler, N., Kemter, K., Richter, G., Cushman, M., and Bacher, A. (2001). Domain structure of riboflavin synthase. Eur. J. Biochem. *268*, 4315–4323.

Gerhardt, S., Schott, A.K., Kairies, N., Cushman, M., Illarionov, B., Eisenreich, W., Bacher, A., Huber, R., Steinbacher, S., and Fischer, M. (2002). Studies on the reaction mechanism of riboflavin synthase: X-ray crystal structure of a complex with

6-carboxyethyl-7-oxo-8-ribityllumazine. Structure *10*, 1371–1381.

Giglione, C., Boularot, A., and Meinnel, T. (2004). Protein N-terminal methionine excision. Cell. Mol. Life Sci. *61*, 1455–1474.

Harvey, R.A., and Plaut, G.W. (1966). Riboflavin synthetase from yeast. Properties of complexes of the enzyme with lumazine derivatives and riboflavin. J. Biol. Chem. *241*, 2120–2136.

Illarionov, B., Eisenreich, W., and Bacher, A. (2001a). A pentacyclic reaction intermediate of riboflavin synthase. Proc. Natl. Acad. Sci. USA *98*, 7224–7229.

Illarionov, B., Kemter, K., Eberhardt, S., Richter, G., Cushman, M., and Bacher, A. (2001b). Riboflavin synthase of *Escherichia coli*. Effect of single amino acid substitutions on reaction rate and ligand binding properties. J. Biol. Chem. *276*, 11524–11530.

Illarionov, B., Haase, I., Bacher, A., Fischer, M., and Schramek, N. (2003). Presteady-state kinetic analysis of riboflavin synthase. J. Biol. Chem. *278*, 47700–47706.

Kuzmic, P. (1996). Program DYNAFIT for the analysis of enzyme kinetic data: application to HIV proteinase. Anal. Biochem. *237*, 260–273.

Liao, D.I., Wawrzak, Z., Calabrese, J.C., Viitanen, P.V., and Jordan, D.B. (2001). Crystal structure of riboflavin synthase. Structure *9*, 399–408.

Meining, W., Eberhardt, S., Bacher, A., and Ladenstein, R. (2003). The structure of the N-terminal domain of riboflavin synthase in complex with riboflavin at 2.6 Å resolution. J. Mol. Biol. *331*, 1053–1063.

Paterson, T., and Wood, H.C.S. (1969). Deuterium exchange of C-methyl protons in 6,7-dimethyl-8-D-ribityl-lumazine, and studies of the mechanism of riboflavine biosynthesis. Chem. Commun. *1969*, 290–291.

Paterson, T., and Wood, H.C. (1972). The biosynthesis of pteridines. VI. Studies of the mechanism of riboflavin biosynthesis. J. Chem. Soc. *8*, 1051–1056.

Plaut, G.W.E. (1963). Studies on the nature of the enzymic conversion of 6,7-dimethyl-8-ribityllumazine to riboflavin. J. Biol. Chem. *238*, 2225–2243.

Plaut, G.W.E., and Beach, R. (1967). In: Flavins and Flavoproteins, T.P. Singer, ed. (Amsterdam, The Netherlands: Elsevier), pp. 737–746.

Plaut, G.W., Smith, C.M., and Alworth, W.L. (1974). Biosynthesis of water-soluble vitamins. Annu. Rev. Biochem. *43*, 899–922.

Römisch, W., Eisenreich, W., Richter, G., and Bacher, A. (2002). Rapid one-pot synthesis of riboflavin isotopomers. J. Org. Chem. *67*, 8890 8894.

Rowan, T., and Wood, H.C.S. (1963). The biosynthesis of riboflavin. Proc. Chem. Soc. 21–22.

Rowan, T., and Wood, H.C. (1968). The biosynthesis of pteridines. V. The synthesis of riboflavin from pteridine precursors. J. Chem. Soc. *4*, 452–458.

Schott, K., Kellermann, J., Lottspeich, F., and Bacher, A. (1990). Riboflavin synthases of *Bacillus subtilis*. Purification and amino acid sequence of the a subunit. J. Biol. Chem. *265*, 4204–4209.

Sedlmaier, H., Müller, F., Keller, P.J., and Bacher, A. (1987). Enzymatic synthesis of riboflavin and FMN specifically labeled with $^{13}C$ in the xylene ring. Z. Naturforsch. C *42*, 425–429.

Truffault, V., Coles, M., Diercks, T., Abelmann, K., Eberhardt, S., Lüttgen, H., Bacher, A., and Kessler, H. (2001). The solution structure of the N-terminal domain of riboflavin synthase. J. Mol. Biol. *309*, 949–960.

Received September 19, 2004; accepted December 5, 2004